Experimental model of primary intraocular lymphoma based on BALB/CaNn strain and A20 cells is optimal for investigational research

Eva Skrlova[1], Eva Uherkova[1], Aneta Klimova[1], Diana Malarikova[2,3], Petra Svozilkova[1], Petr Matous[4], Vit Herynek[4], Tomas Kucera[5], Pavel Klener[2,3], Jarmila Heissigerova[1]

Aim. The purpose of this project was to compare the characteristics of two experimental murine models of primary intraocular lymphoma (PIOL) and determine which experimental model is most suitable for further investigational research to elucidate the pathophysiology of PIOL and to find new therapeutical strategies.
Methods. In both experimental models PIOL was induced in immunocompetent mice with intravitreal injection of syngeneic B-cell lymphoma cell lines. Murine strain C3H/HeN and cell line 38C13 were used in the first model and BALB/CaNn mice and cell line A20 in the second model. During the experiments, thorough clinical evaluation (using photo documentation, ultrasonography, and MRI) and histological evaluation were performed.
Results. In both models, the percentage of PIOL development was high, reaching nearly 80%. Disease progression was faster in C3H/HeN with exophthalmos occurring on average on day 10. Vitreous involvement was a predominant sign in the clinical presentation of this group. In BALB/CaNn mice exophthalmos occurred on average on day 22. The predominant clinical sign in the BALB/CaNn group was tumorous infiltration of the retina, optic disc, and tumorous retinal detachment.
Conclusion. Slower progression of the disease in BALB/CaNn mice, greater possibility to examine the retina due to mild vitreous involvement, and later occurrence of exophthalmos makes this strain more suitable for further investigational research.

Key words: primary intraocular lymphoma, murine experimental models, A20, 38C13

Received: July 26, 2023; Revised: December 11, 2023; Accepted: February 8, 2024; Available online: February 26, 2024
https://doi.org/10.5507/bp.2024.003

[1]Department of Ophthalmology, First Faculty of Medicine, Charles University and General University Hospital, Prague, Czech Republic
[2]Institute of Pathological Physiology, First Faculty of Medicine, Charles University, Prague, Czech Republic
[3]1st Department of Medicine, Department of Haematology, First Faculty of Medicine, Charles University and General University Hospital, Prague, Czech Republic
[4]Centre for Advanced Preclinical Imaging, First Faculty of Medicine, Charles University, Prague, Czech Republic
[5]Institute of Histology and Embryology, First Faculty of Medicine, Charles University, Prague, Czech Republic
Corresponding author: Aneta Klimova, e-mail: aneta.klimova@volny.cz

INTRODUCTION

Lymphomas are a heterogeneous group of cancers originating from cells of the immune system – lymphocytes. They can be divided into two main groups: Hodgkin and non-Hodgkin. The latter is further divided into B-cell and T-cell lymphomas according to the cell of origin. Primary intraocular lymphoma (PIOL) is an uncommon form of non-Hodgkin lymphoma and a subtype of primary central nervous system lymphoma (PCNSL). PIOL makes up 4–6% of all PCNSL (ref.[1]). The type of PIOL is most often (in >95%) diffuse large B-cell lymphoma (DLBCL). The incidence rises over time and is approximately 0.047 cases per 100,000 people per year[1]. The median age of this disease is 50–60 years, with a range from 15 to 85 (ref.[2]). PIOL is an aggressive disease with a poor prognosis. One third of patients diagnosed with intraocular lymphoma already have CNS involvement and 42% to 92% develop CNS involvement between 8–29 months from diagnosis of PIOL (ref.[3]). The clinical picture can vary and often mimics intraocular inflammation. Diagnosis is therefore difficult and may delay effective targeted therapy of this life-threatening disease. Patients with PIOL are usually treated with systemic and intravitreal chemo- and immunotherapy in cooperation with haemato-oncologists. However, the approach to treatment is not uniform and according to data from the world literature, patients are often treated solely locally. The systemic approach prevents earlier relapses and CNS involvement compared with local therapy. Nonetheless, the difference in overall survival is not statistically significant between these treatment modalities[1,4].

Since PIOL is such a rare entity and the amount of intraocular fluid and samples for examination are very limited, studying these tumours is quite challenging. Animal models represent relevant tools for preclinical and translational study of PIOL pathophysiology and proof-of-concept assessment of innovative therapeutical strategies.

First murine lymphoma models used intraperitoneal T-cell lymphoma injections, and then PIOL experimental models were established by intravitreal T-cell inoculation. More recent murine models use B-cell lymphomas

to mimic the true nature and features of lymphomas in humans[5]. According to the literature, several experimental PIOL models have been developed. Most preclinical therapeutic studies have been implemented on a panel of cell line- or patient-derived xenografts in immunodeficient animals[6,7]. However, immunodeficient animal models, by definition, lack specific immunity, which prevents relevant testing of novel immunotherapy approaches (e.g. checkpoint inhibitors, bispecific antibodies) or study of the role of the microbiome in the pathogenesis of PIOL and therapy resistance. In recent years, the microbiome has been shown to play an important role in the development and progression of many diseases, such as multiple sclerosis[8], heart failure[9], depression and anxiety[10], and intraocular inflammation[11]. More importantly, the microbiome has also an undisputable role in response to cancer immunotherapy[12,13]. To study further the role of the microbiome in PIOL development and its response to immunotherapy, we have successfully established two models of PIOL that closely mimic PIOL in humans by intravitreal injections of B-cell lymphoma cells in immunocompetent mice.

METHODS

Animals

Fifty-nine of inbred female mice of C3H/HeN and twenty-four of BALB/CaNn aged 6–10 weeks and weighing 17–22 g were used. Animals had unrestricted access to food and drink and were housed in a menagerie with a 12-hour light/dark cycle. The use of animals for these experiments was approved by the Commission for Animal Welfare of the First Faculty of Medicine, Charles University, Prague, Czech Republic, and the Ministry of Education, Youth and Sports according to animal protection laws. All the procedures were approved by the animal experimentation review committee under number MSMT-29413/2020-6.

Induction of PIOL in C3H/HeN

The 38C13 cell line was used to induce PIOL in the C3H/HeN mice strain. The 38C13 cells were originally induced by carcinogens in T-cell-depleted mice of the C3H/HeN strain. 38C13 cells express IgM/k on their surface, however, they do not secrete it. 38C13 cells are MHC I+, MHC II– (ref.[14]).

The 38C13 cells were always prepared immediately before the application from pre-grown subcutaneous tumours. The tumour was then passaged, diluting the cells in phosphate-buffered saline (PBS) at the desired concentration. The application took place within 2–3 hours post-preparation. The viability of the cells was checked in the remaining solution after application and no decrease in the concentration of viable tumour cells was detected. As in the experimental model of autoimmune uveitis[15], the induction was not straightforward and without problems. In vitro cultivated cells were not viable enough to induce PIOL and cells from subcutaneous tumour needed to be resuspended before each application in order to induce PIOL.

Induction of PIOL was performed by intravitreal injection with a 33G needle of 1µL of a suspension of 38C13 cells in PBS at a concentration of 500,000–750,000 cells/mL. The instruments were disinfected with povidone iodinate solution and washed with sterile distilled water before each injection. The operative field was disinfected for 1 min with a 2% chlorhexidine solution and rinsed with sterile distilled water. The procedure was performed under general anaesthesia with isoflurane under microscopic control in one eye only at a time. The suspension of tumour cells was applied for 1 min. The needle was further left in the wound for 1 min before removal to reduce the reflux of cancer cells.

Induction of PIOL in BALB/CaNn

The A20 cell line was used to induce PIOL in BALB/CaNn mice. This cell line of B-cell lymphoma was derived from a spontaneous reticulum cell neoplasm found in an old BALB/CaNn mouse[16].

A20 cells were cultured in vitro in Iscove's modified Dulbecco's media with 10% foetal bovine serum/foetal calf serum and just before application diluted in PBS at the desired concentration. The viability of these cells was checked in the remaining solution after application and

Table 1. Clinical scoring system.

Keratic precipitates score 0–2		Iris infiltration score 0–2		Exophthalmos score 0–5		Retina score 0–4		Vitreous score 0–5	
0	none	0	none	0	none	0	no pathological finding	0	no pathological finding
1	mild	1	mild	10	exophthalmos with intact anterior segment	1	vessel involvement	1	mild
2	severe	2	severe	15	exophthalmos with destruction of anterior segment	1	retinal infiltration	3	moderate
						1	retinal detachment	5	severe, no structures of retina visible
						1	optic disc infiltration		

no decrease in the concentration of viable tumour cells was detected.

Induction of PIOL was performed by intravitreal injection with a 33G needle of 1µL of a suspension of A20 cells in PBS at a concentration of 750,000–1,250,000 cells/mL. The following procedure was identical to that of the C3H/Hen strain as listed above.

Clinical follow-up after induction of PIOL

The development of PIOL was checked at regular intervals twice a week. The clinical in vivo examination (bio-microscopy) was performed using a modified camera system with an otoscope. An additional +4 dioptre lens between the camera and otoscope was used[17]. The clinical appearance was then assessed by a scoring system (Table 1), which was introduced based on the data from the literature and modified according to our clinical experience[18]. If possible, the evaluation was performed by two persons to reduce possible bias and error. Furthermore, MRI and ultrasound imaging methods (Fig. 1, Fig. 2) were used in selected cases to monitor extraocular and intraocular propagation. Animals were scanned on two MR scanners (a 7 T scanner was not available at the beginning of the experiment). Initial MR scanning was performed on an ICON MR tomograph (Bruker, Ettlingen, Germany) at a magnetic field of 1 T equipped with a solenoid mouse head coil using standard turbospin echo sequences. Sequences covered the frontal part of the brain with eyes in axial and coronal directions. Later experiments were continued using a 7T MR scanner MRS*DRYMAG 7.0T (MR Solutions, Guildford, United Kingdom) equipped with a mouse head resonator coil. T2-weighted turbospin echo sequences covering the same area (frontal part of the brain with eyes in axial and coronal directions) were acquired. Ultrasound images were acquired using a preclinical imaging platform Vevo 3100/

Table 2. The affinity of lymphoma cells to ocular and periocular tissue.

38C13 cell affinity	A20 cell affinity
vitreous	vitreous
subretinal space	retina
anterior chamber structures	anterior chamber structures
orbit	ciliary body
	iris
	choroid

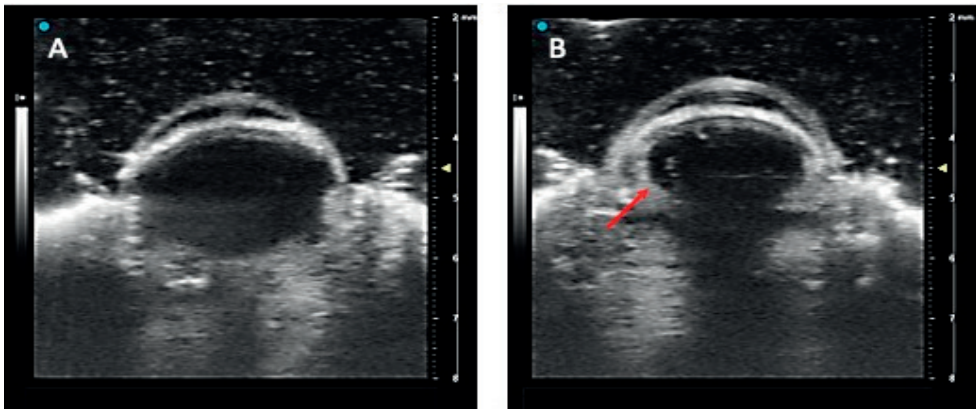

Fig. 1. Ultrasound.
A. healthy eye; **B.** eye with PIOL; vitreous infiltration (red arrow).

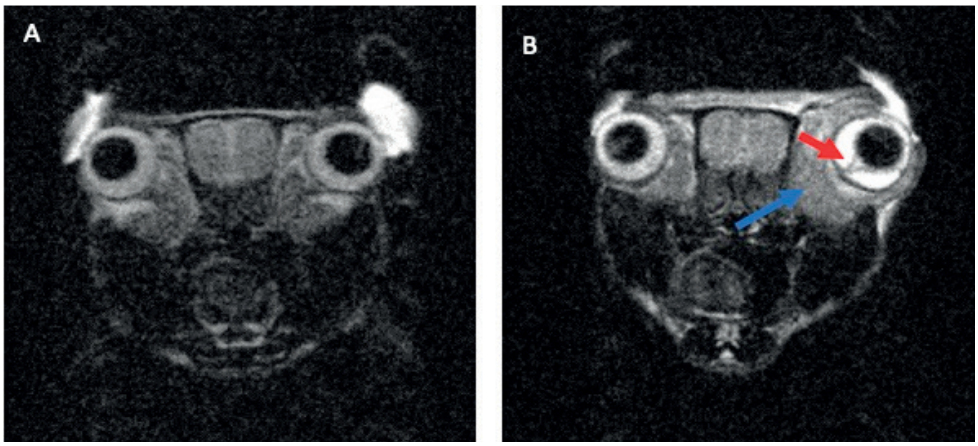

Fig. 2. MRI.
A. no orbital involvement; **B.** tumorous orbital infiltration (blue arrow); retinal detachment (red arrow).

LAZR-X (Fujifilm VisualSonics, Toronto, ON, Canada) equipped with an MX700 transducer (30–70 MHz, axial resolution 30 μm).

For intravitreal application, clinical examination, MRI, and US, mice were anaesthetised by isoflurane (3% for induction, 1.5–2% for maintenance) and kept on a heated bed or pad during the measurement. Vital functions were monitored during the scanning.

The experiment was terminated at the first sign of exophthalmos. Animals were sacrificed according to the ethical rules given by the law of the Czech Republic by cervical dislocation.

Tissue processing for immunohistochemistry

Eyeballs were harvested post-mortem, immediately immersed in Tissue-Tek® O.C.T. Compound™ (Sakura Finetek, Inc., Torrance, CA), and fresh frozen in 2-methylbutane (Sigma-Aldrich, St. Louis, MO) in liquid nitrogen. Samples were stored at −80 °C. Then they were cut into 7 μm thick sagittal sections and stained. To further study the involvement of the ocular tissues and to prove the presence of lymphoma cells sections were stained with rat anti-mouse CD19 monoclonal antibody (6OMP31, eBioscience™, Invitrogen) diluted 1:100 in 1.5% goat serum. Visualization of primary antibody binding was performed using a biotinylated secondary goat anti-rat biotin and avidin-biotin-peroxidase complex. Diaminobenzidine was used as a substrate and sections were stained with hematoxylin.

Data analysis

Data were analysed using GraphPad Prism Version 8.01 for Windows (GraphPad Software, San Diego, CA, http://www.graphpad.com). Kruskal-Wallis and Mann-Whitney nonparametric tests were used to evaluate differences between the groups. The *P* value of <0.05 was considered significant.

RESULTS

Both mice strains showed a high percentage of PIOL development. C3H/Hen strain reached 78% (46 from 59 eyes) and BALB/CaNn 79% (19 from 24 eyes). Clinical signs of PIOL were keratic precipitates, iris infiltration, vitreous infiltration, retinal infiltration or retinal detachment, vessel involvement, and optic disc infiltration.

In the C3H/HeN strain, the lymphoma progressed faster with the average length of the experiment being 10 days. The predominant sign of PIOL in this group was vitreous involvement (Fig. 3.) The exophthalmos in C3H/HeN occurred on average on day 10 (between days 7–21). In contrast, experiments with BALB/CaNn strain had a longer duration and were terminated on day 30 as the disease progressed slowly and it may take up to 56 days before exophthalmos occurs (only the first experiment was terminated on day 56 to establish characteristics of the lymphoma development). In BALB/CaNn mice strain exophthalmos started to appear on average on day 22 (between days 14–56). 2 mice with histologi-

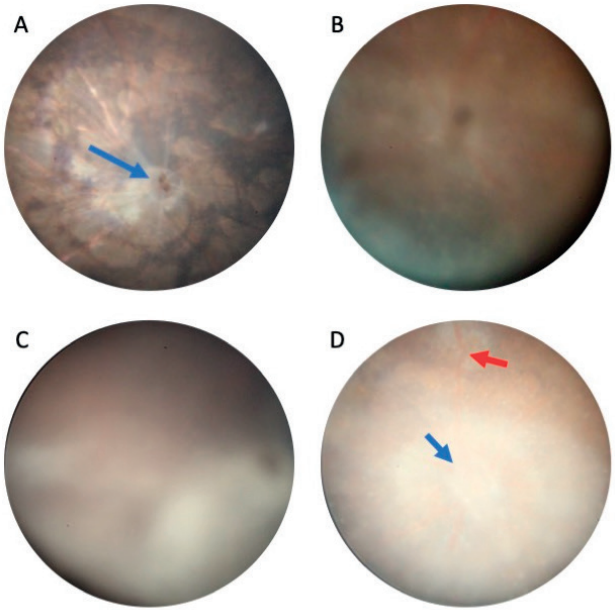

Fig. 3. Signs of primary intraocular lymphoma in C3H/HeN mice.
A. physiological fundus photography, optic disc (blue arrow); **B.** mild vitreous infiltration; **C.** severe vitreous infiltration; **D.** tumorous infiltration of the retina (red arrow), tumorous infiltration of the optic disc (blue arrow).

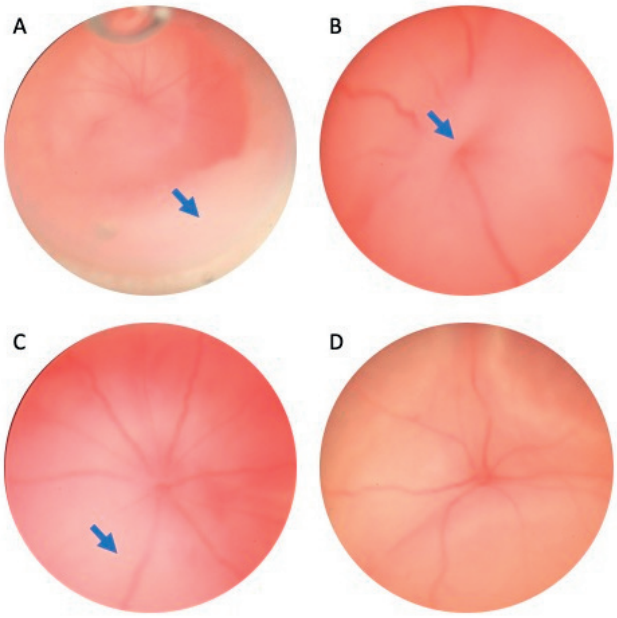

Fig. 4. Signs of primary intraocular lymphoma in BALB/CaNn mice.
A. keratic precipitates forming plaques on the endothelium (star); **B.** optic disc infiltration (blue arrow); **C.** retinal infiltration; **D.** tumorous retinal detachment.

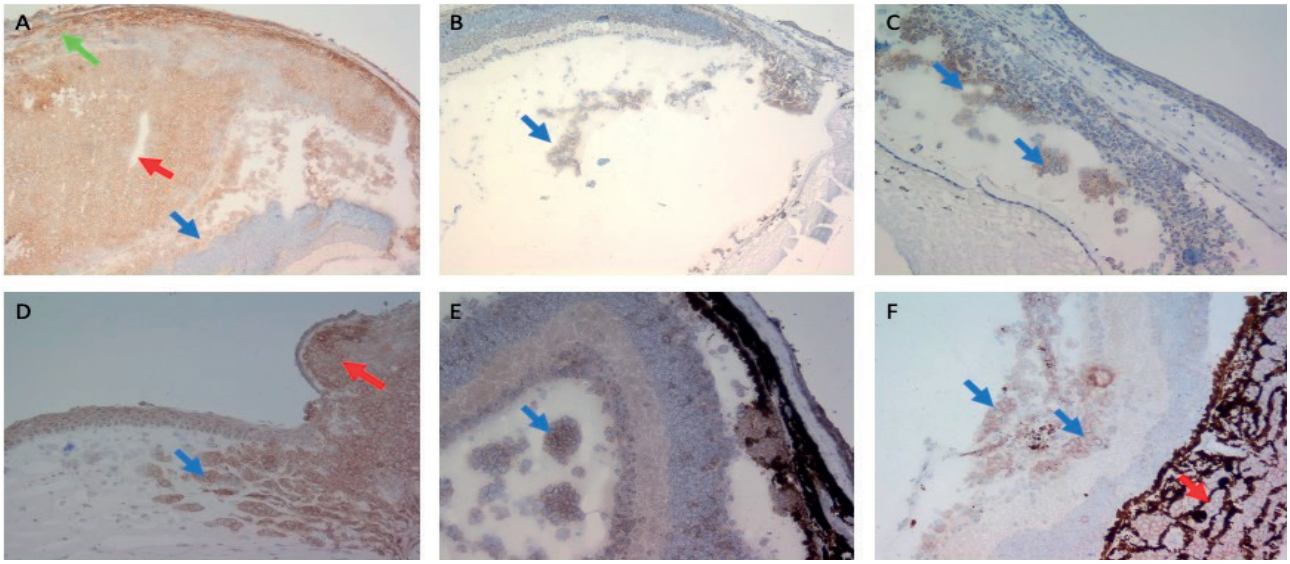

Fig. 5. Immunohistochemistry – CD19 antibody labels 38C13 and A20 cell membranes.
A. BALB/CaNn massive infiltration of subretinal space (red arrow), tumorous retinal detachment (blue arrow), scleral destruction (green arrow); B. BALB/CaNn vitreous infiltration (blue arrow); **C.** BALB/CaNn anterior chamber infiltration (blue arrows); **D.** C3H/HeN corneal (blue arrow) and conjunctival (red arrow) infiltration; **E.** C3H/HeN vitreous infiltration (blue arrow); **F.** C3H/HeN retinal infiltration (blue arrows) and choroidal destruction (red arrow).

cally proven PIOL did not develop exophthalmos at all. In BALB/CaNn strain the predominant clinical signs of PIOL were tumorous infiltration of the retina, tumorous infiltration of the optic disc, and tumorous retinal detachment (Fig. 4). Keratic precipitates and iris infiltration occurred to a lesser extent in both strains and the intensity occasionally fluctuated over the course of the experiment in the same individual.

The difference in the rate of PIOL progression is demonstrated in Fig. 6. The difference between the clinical scores of C3H/HeN and BALB/CaNn was statistically significant on day 3 (P<0.05), day 7 (P<0.0001), day 10 (P<0.0001), day 14 (P<0.05). This outlined a significantly higher rate of progression in C3H/HeN mice, with first signs of lymphoma apparent from day 3 after application in most mice. This is in contrast to BALB/CaNn mice, where the clinical manifestation of lymphoma was apparent on day 3 in some cases, but most mice showed some PIOL signs on day 10.

Cerebral infiltration was not proved in individual cases that were examined by MRI. No lymphoma spread to the fellow eyes was observed in either group.

Histological findings were consistent with the clinical presentation of PIOL in both groups. Based on the severity of clinical appearance lymphoma cells were found in the cornea, anterior chamber, iris, vitreous, retina, choroid, sclera, and periocular tissues (Fig. 5). Infiltration of conjunctiva around the injection site was often observed because of reflux of lymphoma cells. Furthermore, infiltration of the choroid was often more pronounced in the area adjacent to the injection site. Isolated extraocular development as the only clinical manifestation of lymphoma was detected in 9 cases of C3H/HeN strain.

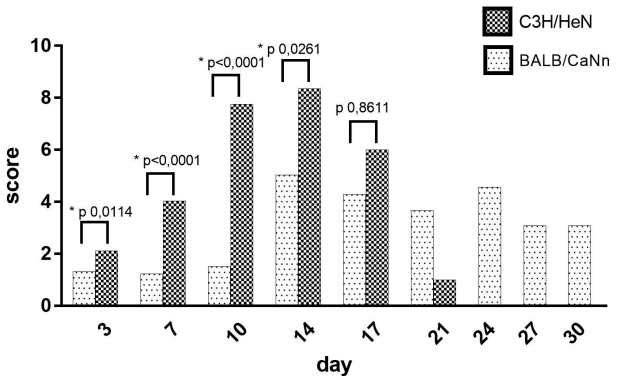

Fig. 6. Comparison of mean score of two models in time. The graph demonstrates the difference between mean score values in time in two mice strains. C3H/HeN mice have a higher score from the beginning. In BALB/CaNn strain the progression of PIOL is slower. There is a statistically significant difference between the scores on days 3, 7, 10, and 14. On day 17 the difference is diminished due to the more frequent appearance of exophthalmos in the BALB/CaNn group.

DISCUSSION

In this study, we introduced and characterized two murine models of immunocompetent animal PIOL by transplantation of syngeneic murine lymphoma cell line into their respective syngeneic murine strains. The lymphoma induced by A20 and 38C13 cell intravitreal injections primarily developed in the vitreous cavity and subretinal space (based on histological evaluation and clinical presentation) as was shown in previous experiments[19]. This location of tumour cells is characteristic of the human PIOL (ref.[20]). Cancer cells were also found in the

iris, anterior chamber, on the corneal endothelium, and in advanced cases in the cornea itself as was described in previous works[16]. In contrast to our experience, the authors used higher concentrations of A20 cells (10^4). We observed infiltration of the anterior segment of the eye even with a lower concentration (10^3) of lymphoma cells. The clinical scoring system is most helpful in PIOL assessment[18]. However, some experience is needed, and it is burdened by human error since it is subjective. Also, some features in the clinical picture varied over time. For example, diffuse keratic precipitates, sometimes forming plaques, were observed during the first days and their intensity fluctuated. In some cases, keratic precipitates spontaneously resolved, but lymphoma cells were still found in the anterior chamber on histological sections. The spontaneous resolution of keratic precipitates was not described by other authors. Posterior synechiae were also frequently observed in the C3H/HeN strain. Since posterior synechiae are not typical of PIOL in humans and this complication has not been described by other authors using the C3H/HeN mouse strain-based PIOL, this raises the question of whether some of the features may also be inflammatory after application.

In our experiments, both murine strains show a high percentage of PIOL development. In the C3H/HeN strain, the progression of the disease is faster with earlier development of exophthalmos in contrast to the BALB/CaNn strain where the progression is significantly slower. Earlier development of exophthalmos in C3H/HeN mice is most likely due to the difference in lymphoma cells' affinity to orbital tissue. 38C13 cell line used in C3H/HeN mice has a primary affinity to orbital tissue contrary to A20 cells (Table 2) (ref.[21]). Despite the slow application, we were not able to avoid the reflux of lymphoma cells, which could then directly infiltrate tissues outside the target site such as conjunctiva or orbital tissue. This explanation is also supported by the cases where no intraocular infiltration was histologically proven despite exophthalmos development. In some histological sections of the eyes of the C3H/HeN mice strain, it was also difficult to distinguish whether the lymphoma propagated from the vitreous, infiltrated the sclera, and subsequently migrated to the orbit, or whether the primary infiltration occurred in the orbit and the bulbus was destroyed from external lymphoma infiltration. Similar problems were not described by other authors using murine PIOL models.

CONCLUSION

With all the limitations presented by the artificial induction of PIOL, the model using immunocompetent animals is crucial for studying and understanding this rare disease and its influencing factors. Based on our experience, BALB/CaNn mice with A20 cell inoculation will be more suitable for therapeutic experiments since the progression of the disease is slower. In addition, A20 cells do not have a primary affinity to orbital tissue hence the exophthalmos appears to occur mostly due to the propagation of PIOL through the sclera and not by accidental dissemination of lymphoma cells during intravitreal application. Last but not least, is also the fact that in BALB/CaNn mice vitreous involvement is almost always mild, which allows better visualization of the fundus and more precise score assessment. This will be important in therapeutic trials and evaluation of therapy effectiveness.

Acknowledgments: This study was supported by the research project from the Ministry of Health of the Czech Republic AZV NU 20-03-00253 and by the Charles University Institutional Programme SVV 260631. The infrastructure of the core facility Centre for Advanced Preclinical Imaging, First Faculty of Medicine, Charles University, was supported by the MEYS CR (LM2023050 Czech-BioImaging), and by European Regional Development Fund (Project CZ.02.1.01/0.0/0.0/18_046/0016045).

We would like to thank Prof. J. Kovar, 3rd Faculty of Medicine, for the generous donation of the 38C13 cell line, and RE Davis (The UT MDACC) for the generous donation of the A20 cell line.

Author contributions: ES, EU: design and execution of experiments, results interpretation; AK: supervision and consultation of results; DM: lymphoma cell preparation; PS: design of experiments, supervision; PM, VH: MRI and US (conduct of the examination and interpretation of results); TK: consultation and supervision of histological evaluation; PK, JH: design of experiments, consultation of results.

Conflict of interest statement: None.

REFERENCES

1. Venkatesh R, Bavaharan B, Mahendradas P, Yadav NK. Primary vitreoretinal lymphoma: prevalence, impact, and management challenges. Clin Ophthalmol 2019;13:353-64.
2. Tang LJ, Gu CL, Zhang P. Intraocular lymphoma. Int J Ophthalmol 2017;10(8):1301-7.
3. Sagoo MS, Mehta H, Swampillai AJ, Cohen VM, Amin SZ, Plowman PN, Lightman S. Primary intraocular lymphoma. Surv Ophthalmol 2014;59(5):503-16.
4. Klimova A, Heissigerova J, Rihova E, Brichova M, Pytlik R, Spicka I, Mrazova K, Karolova J, Svozilkova P. Combined treatment of primary vitreoretinal lymphomas significantly prolongs the time to first relapse. Br J Ophthalmol 2018;102(11):1579-85.
5. Chan CC, Fischette M, Shen D, Mahesh SP, Nussenblatt RB, Hochman J. Murine model of primary intraocular lymphoma. Invest Ophthalmol Vis Sci 2005;46(2):415-9. doi: 10.1167/iovs.04-0869
6. Jakša R, Karolová J, Svatoň M, Kazantsev D, Grajciarová M, Pokorná E, Tonar Z, Klánová M, Winkowska L, Maláriková D, Vočková P, Forsterová K, Renešová N, Dolníková A, Nožičková K, Dundr P, Froňková E, Trněný M, Klener P. Complex genetic and histopathological study of 15 patient-derived xenografts of aggressive lymphomas. Lab Invest 2022;102(9):957-65.
7. Zhang L, Nomie K, Zhang H, Bell T, Pham L, Kadri S, Segal J, Li S, Zhou S, Santos D, Richard S, Sharma S, Chen W, Oriabure O, Liu Y, Huang S, Guo H, Chen Z, Tao W, Li C, Wang J, Fang B, Wang J, Li L, Badillo M, Ahmed M, Thirumurthi S, Huang SY, Shao Y, Lam L, Yi Q, Wang YL, Wang M. B-Cell Lymphoma Patient-Derived Xenograft Models Enable Drug Discovery and Are a Platform for Personalized Therapy. Clin Cancer Res 2017;23(15):4212-23.
8. Rebeaud J, Peter B, Pot C. How Microbiota-Derived Metabolites Link the Gut to the Brain during Neuroinflammation. Int J Mol Sci 2022;23(17):10128. doi: 10.3390/ijms231710128

9. Tang WHW, Li DY, Hazen SL. Dietary metabolism, the gut microbiome, and heart failure. Nat Rev Cardiol 2019;16(3):137-54.
10. Aslam H, Green J, Jacka FN, Collier F, Berk M, Pasco J, Dawson SL. Fermented foods, the gut and mental health: a mechanistic overview with implications for depression and anxiety. Nutr Neurosci 2020;23(9):659-71.
11. Dusek O, Fajstova A, Klimova A, Svozilkova P, Hrncir T, Kverka M, Coufal S, Slemin J, Tlaskalova-Hogenova H, Forrester JV, Heissigerova J. Severity of Experimental Autoimmune Uveitis Is Reduced by Pretreatment with Live Probiotic Escherichia coli Nissle 1917. Cells 2020;10(1):23. doi: 10.3390/cells10010023
12. Li W, Deng Y, Chu Q, Zhang P. Gut microbiome and cancer immunotherapy. Cancer Lett 2019;447:41-7.
13. Yi M, Jiao D, Qin S, Chu Q, Li A, Wu K. Manipulating Gut Microbiota Composition to Enhance the Therapeutic Effect of Cancer Immunotherapy. Integr Cancer Ther 2019;18:1534735419876351.
14. Muraro S, Bondanza A, Bellone M, Greenberg PD, Bonini C. Molecular modification of idiotypes from B-cell lymphomas for expression in mature dendritic cells as a strategy to induce tumor-reactive CD4+ and CD8+ T-cell responses. Blood 2005;105(9):3596-3604.
15. Klimova A, Seidler Stangova P, Svozilkova P, Kucera T, Heissigerova J. The Clinical Signs of Experimental Autoimmune Uveitis. Cesk Slov Oftalmol 2016;72(1):276-82.
16. Touitou V, Daussy C, Bodaghi B, Camelo S, de Kozak Y, Lehoang P, Naud MC, Varin A, Thillaye-Goldenberg B, Merle-Béral H, Fridman WH, Sautès-Fridman C, Fisson S. Impaired th1/tc1 cytokine production of tumor-infiltrating lymphocytes in a model of primary intraocular B-cell lymphoma. Invest Ophthalmol Vis Sci 2007;48(7):3223-9.
17. Seidler Stangova P, Dusek O, Klimova A, Heissigerova J, Kucera T, Svozilkova P. Metronidazole Attenuates the Intensity of Inflammation in Experimental Autoimmune Uveitis. Folia Biol (Praha) 2019;65(5-6):265-74.
18. Mineo JF, Scheffer A, Karkoutly C, Nouvel L, Kerdraon O, Trauet J, Bordron A, Dessaint JP, Labalette M, Berthou C, Labalette P. Using human CD20-transfected murine lymphomatous B cells to evaluate the efficacy of intravitreal and intracerebral rituximab injections in mice. Invest Ophthalmol Vis Sci 2008;49(11):4738-45.
19. Ben Abdelwahed R, Donnou S, Ouakrim H, Crozet L, Cosette J, Jacquet A, Tourais I, Fournès B, Gillard Bocquet M, Miloudi A, Touitou V, Daussy C, Naud MC, Fridman WH, Sautès-Fridman C, Urbain R, Fisson S. Preclinical study of Ublituximab, a Glycoengineered anti-human CD20 antibody, in murine models of primary cerebral and intraocular B-cell lymphomas. Invest Ophthalmol Vis Sci 2013;54(5):3657-65.
20. Gunduz K, Pulido JS, McCannel CA, O'Neill BP. Ocular manifestations and treatment of central nervous system lymphomas. Neurosurg Focus 2006;21(5):E9.
21. Aronow ME, Shen D, Hochman J, Chan CC. Intraocular Lymphoma Models. Ocul Oncol Pathol 2015;1(3):214-22.